

## Fermi Surface Properties of $\text{CeRu}_2(\text{Si}_{1-x}\text{Ge}_x)_2$ in Magnetic Fields above the Metamagnetic Transitions

M. Sugi,<sup>1</sup> Y. Matsumoto,<sup>1</sup> N. Kimura,<sup>1</sup> T. Komatsubara,<sup>1</sup> H. Aoki,<sup>1</sup> T. Terashima,<sup>2</sup> and S. Uji<sup>2</sup>

<sup>1</sup>Graduate School of Science and Center for Low Temperature Science, Tohoku University, Miyagi 980-8577, Japan

<sup>2</sup>National Institute for Materials Science, Ibaraki 305-0044, Japan

(Received 16 July 2007; published 29 July 2008)

We report de Haas–van Alphen effect measurements on  $\text{CeRu}_2(\text{Si}_{1-x}\text{Ge}_x)_2$  to reveal electronic structure change over the broad range of chemical pressure from  $x = 0.0$  to 1.0. It is found that the Fermi surface properties change drastically across the metamagnetic crossover field ( $B_m$ ) but vary smoothly with  $x$  from those in magnetic fields above  $B_m$  in  $\text{CeRu}_2\text{Si}_2$  to those in the ferromagnetic state in  $\text{CeRu}_2\text{Ge}_2$ . Implications of the present results are discussed in conjunction with the magnetic phase diagram.

DOI: 10.1103/PhysRevLett.101.056401

PACS numbers: 71.18.+y, 71.27.+a, 75.20.Hr

Most interesting properties of the strongly correlated  $f$  electron systems arise from the nearly localized nature of the  $f$  electron. Where and how the  $f$  electron changes its nature from itinerant to localized has been a long standing issue and is currently revived with the progress of the study on the quantum phase transition. Related with this issue, interesting observations were reported for the metamagnetic transition of  $\text{CeRu}_2\text{Si}_2$ .  $\text{CeRu}_2\text{Si}_2$  is a paramagnetic heavy fermion compound and is thought to be situated close to an antiferromagnetic quantum critical point as described below in Fig. 2. When a magnetic field is applied along the  $c$  axis of its  $\text{ThCr}_2\text{Si}_2$  structure, it exhibits metamagnetic transition at 7.7 T. The Fermi surface (FS) changes drastically across the metamagnetic transition field ( $B_m$ ) [1–3]. The effective mass ( $m^*$ ) and the electronic specific heat coefficient are enhanced around  $B_m$ . A simple interpretation of the change was that the  $f$  electron changes its nature from itinerant to localized [1,3]. Figures 1(a) and 1(b) [4,5] show the FS's of  $\text{CeRu}_2\text{Si}_2$  by the band structure calculation when the  $f$  electron is assumed to be itinerant and localized, respectively.

These observations are similar to those observed for the quantum critical point. However, the electronic specific heat coefficient does not diverge and the transition is not phase transition but crossover. It is also reported that around  $B_m$ , the system is not Fermi liquid down to very low temperatures but in the low temperature limit the Fermi liquid behavior recovers [6,7]. In other words the electronic properties seem to change continuously across  $B_m$  and the  $f$  electron may remain itinerant. To obtain deeper insight into this issue, it will be very useful to change the electronic state above  $B_m$  continuously, for example, by pressure, to that where the  $f$  electron is localized without doubt.

We employ chemical pressure, i.e., substitute Si for Ge in  $\text{CeRu}_2\text{Si}_2$ , to expand the lattice or to make the  $f$  electron more localized.  $\text{CeRu}_2(\text{Si}_{1-x}\text{Ge}_x)_2$  is a suitable system because it is established that in  $\text{CeRu}_2\text{Ge}_2$  the  $f$  electron is localized and the previous studies show that applica-

tion of pressure about 11 GPa on  $\text{CeRu}_2\text{Ge}_2$  gives nearly the same magnetic phase diagram with that of  $\text{CeRu}_2(\text{Si}_{1-x}\text{Ge}_x)_2$  as a function of unit cell volume ( $V_u$ ) [8,9]. This fact together with successful observation of the de Haas–van Alphen (dHvA) signals in  $\text{CeRu}_2(\text{Si}_{1-x}\text{Ge}_x)_2$

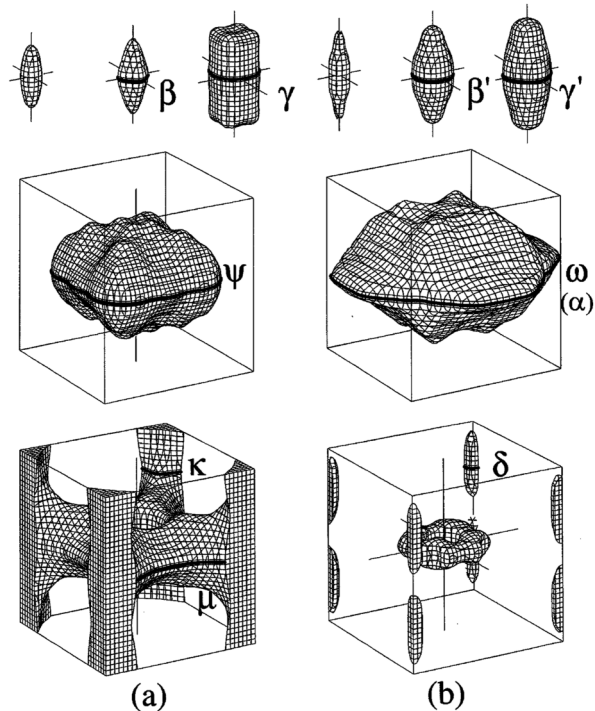


FIG. 1. Fermi surfaces (FS's) of  $\text{CeRu}_2\text{Si}_2$  (a) and  $\text{LaRu}_2\text{Si}_2$  (b). In both the figures the FS's in the top and middle are hole FS's and those in the bottom are electron FS's. The FS of  $\text{CeRu}_2\text{Ge}_2$  or that of the localized  $f$  electron model for  $\text{CeRu}_2\text{Si}_2$  is very similar to that of  $\text{LaRu}_2\text{Si}_2$ . The figures indicate the names of the dHvA oscillations and the corresponding orbits when the field is applied parallel to the  $c$  axis. The oscillation from the orbit on the large hole FS is denoted by  $\omega$  in the case of the localized  $f$  electron model in  $\text{CeRu}_2\text{Si}_2$  and by  $\alpha$  in  $\text{CeRu}_2\text{Ge}_2$ .

in the present study indicates that the substitution gives an almost purely pressure effect without disturbing the electronic properties near the Fermi level. We report the first successful attempt to reveal the electronic structure change via the dHvA effect over the broad range of chemical pressure.

The single crystals were grown by using the Czochralski pulling method in a tetra-arc furnace and were annealed under vacuum for a week at 900 °C.  $V_u$  of each  $\text{CeRu}_2(\text{Si}_{1-x}\text{Ge}_x)_2$  sample was determined by the conventional x-ray diffraction method. For some samples chemical analysis and electron-probe microanalysis (EPMA) were performed to check the composition of the sample. The content  $x$  of Ge was estimated from the  $V_u$  of  $\text{CeRu}_2(\text{Si}_{1-x}\text{Ge}_x)_2$  by assuming that  $V_u$  changes linearly with the Ge concentration and is used to label the sample. dc magnetic measurements were performed by using a commercial SQUID magnetometer. The dHvA effect and ac susceptibility measurements were performed by using the conventional field modulation method in dilution refrigerators under magnetic fields up to 18 T.

Figure 2 shows the magnetic phase diagram of  $\text{CeRu}_2(\text{Si}_{1-x}\text{Ge}_x)_2$  as a function of  $x$  or  $V_u$ . Ferromagnetic transition temperature  $T_c$ , and antiferromagnetic transition temperatures  $T_N$  and  $T_L$  are plotted on the temperature vs  $V_u$  plane. The transition temperatures agree well with the previous results [8].  $T_c$  decreases with decreasing  $V_u$  and vanishes rather rapidly at around  $V_u = 178.6 \text{ \AA}^3$ . With decreasing  $V_u$   $T_N$  increases slightly and then decreases quickly to vanish around the critical volume  $V_{uc} = 172.9 \text{ \AA}^3$ .  $T_m$  is the temperature at the broad maximum of the susceptibility vs temperature curve and is related to the Kondo temperature  $T_K$ . In the present case

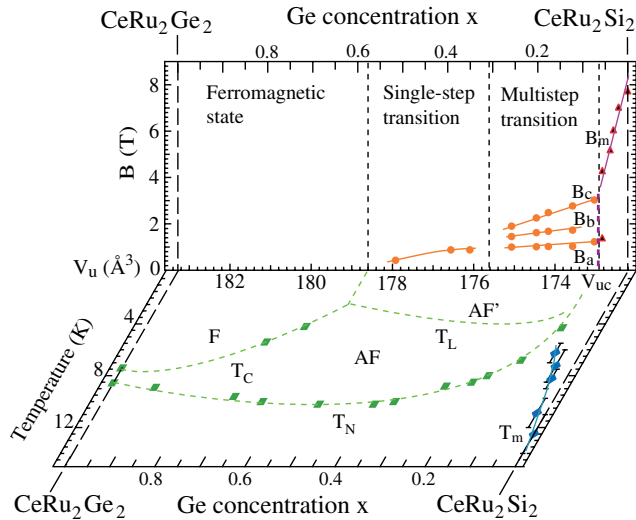


FIG. 2 (color online). Magnetic phase diagram plotted on  $T$  vs  $V_u$  plane and on  $B$  vs  $V_u$  plane with  $B$  parallel to the  $c$  axis. The transition at  $T_L$  can be observed only by the resistivity measurements [8]. The dotted lines are guides for the eye.

it appears that  $T_m \approx T_K/2$ , if  $T_K$  of  $\text{CeRu}_2\text{Si}_2$  is 25 K [10].  $T_m$  decreases with increasing  $V_u$  but remains finite in the vicinity of  $V_{uc}$ .

On the  $B$  vs  $V_u$  plane, we plot metamagnetic transition fields. With increasing  $V_u$  from  $\text{CeRu}_2\text{Si}_2$ , the metamagnetic crossover field  $B_m$  decreases. Around  $V_{uc}$  the metamagnetic crossover changes to weakly first-order metamagnetic transitions at  $B_a$  and  $B_c$  [8,11]. With further increase of  $V_u$ , the two transitions exhibit clearer first-order nature and at lower temperatures below 2 K it becomes obvious that another transition takes place at a field  $B_b$  between  $B_a$  and  $B_c$ . The magnetization curve changes from the multistep transition to the single step transition around  $V_u = 175.6 \text{ \AA}^3$ . The transition field shifts to lower fields with increasing  $V_u$  and finally the system becomes ferromagnetic. Figure 2 indicates that the boundary between the antiferromagnetic and paramagnetic states on the  $B$  vs  $V_u$  plane extends almost vertically from  $V_{uc}$ . The features of the phase boundaries at  $V_{uc}$  on the  $B$  vs  $V_u$  and  $T$  vs  $V_u$  planes may suggest that the antiferromagnetic and paramagnetic phases are separated by first-order phase transition.

We have successfully observed the dHvA oscillations  $\beta'$ ,  $\gamma'$ , and  $\delta$  above  $B_m$  and  $B_c$  as well as in the ferromagnetic state. Figure 3(a) shows examples of the dHvA oscillations and Fourier spectra in the states where the metamagnetic crossover ( $x = 0.03$ ), multistep ( $x = 0.20$ ) and single-step first-order metamagnetic transitions ( $x = 0.39$ ) are observed as well as in the ferromagnetic state ( $x = 0.65$ ). Their frequencies ( $F$ 's) are plotted as a function of  $V_u$  in Fig. 3(b). Each  $F$  changes continuously with decreasing  $V_u$  and splits in the ferromagnetic state. In the FS model for the localized  $f$  electron [Fig. 1(b)], the  $\beta'$  and  $\gamma'$  oscillations are attributed to the hole surfaces and the  $\delta$  oscillation to the electron surface [1,3]. We could not observe the  $\omega$  or  $\alpha$  oscillation in the alloy samples. However, the smooth changes in the  $F$ 's of  $\beta'$ ,  $\gamma'$ , and  $\delta$  strongly indicate that there is not such a drastic FS change as the transition between the FS's of Figs. 1(a) and 1(b) at a particular  $V_u$ . Since the transition of the  $f$  electron nature decreases the number of conduction electrons or reconstructs the FS completely, there should be a discontinuous change in each  $F$ .

Figure 4(a) shows the  $m^*$ 's of the  $\beta'$  oscillations as a function of magnetic field for samples  $x = 0.0$  [1,3], 0.03, 0.06, 0.07, and 0.20. For samples  $x = 0, 0.03$ , and 0.06 where the metamagnetic crossovers are found, the  $m^*$ 's are enhanced around  $B_m$ . There are some dip structures in the measured  $m^*$  vs field curves which deviate from the guide lines. These are artifacts of the analysis arising from the fact that the  $m^*$  depends on the direction of spin as well as on the magnetic field [1,3,12]. For  $x = 0.07$ , there is also significant field dependence of the  $m^*$ . In larger Ge content samples, the field dependence of the  $m^*$  at high fields is small as demonstrated for  $x = 0.20$ . For the  $\gamma'$  and  $\delta$

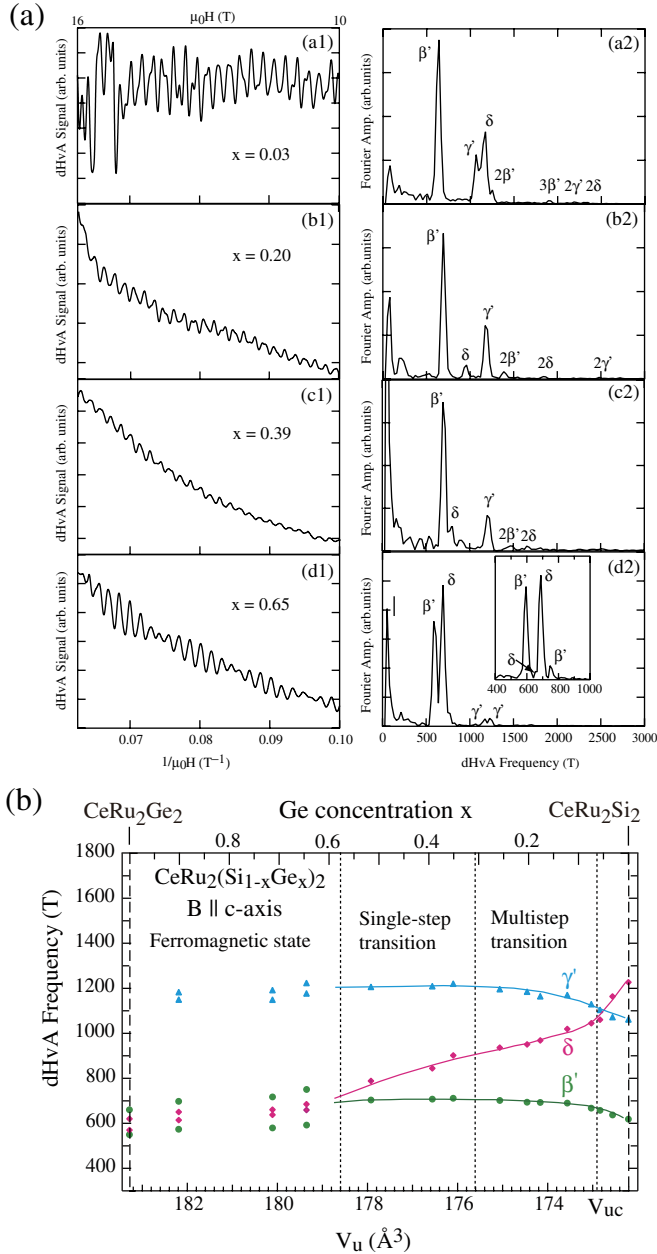


FIG. 3 (color online). (a) DHvA oscillations of CeRu<sub>2</sub>(Si<sub>1-x</sub>Ge<sub>x</sub>)<sub>2</sub> with  $x = 0.03$ (a1),  $0.20$ (b1),  $0.39$  (c1),  $0.65$ (d1) and corresponding Fourier spectra (a2), (b2), (c2), (d2). The inset of (d2) is the Fourier spectrum obtained from the Fourier analysis over wider range between  $17.5$  T and  $8$  T to separate the up and down spin frequencies.  $T < 100$  mK and  $B \parallel c$  axis. (b) DHvA frequencies of the  $\beta'$ ,  $\gamma'$  and  $\delta$  oscillations plotted against  $V_u$  or Ge concentration  $x$ . The solid lines are guides to the eye.

oscillations reliable field dependences could not be obtained because of the lower signal intensities as well as the closeness of the two frequencies as noted from Figs. 3. However, it is very likely that the  $m^*$ 's of these frequencies are also enhanced around  $B_m$  as observed in CeRu<sub>2</sub>Si<sub>2</sub> [1,3].

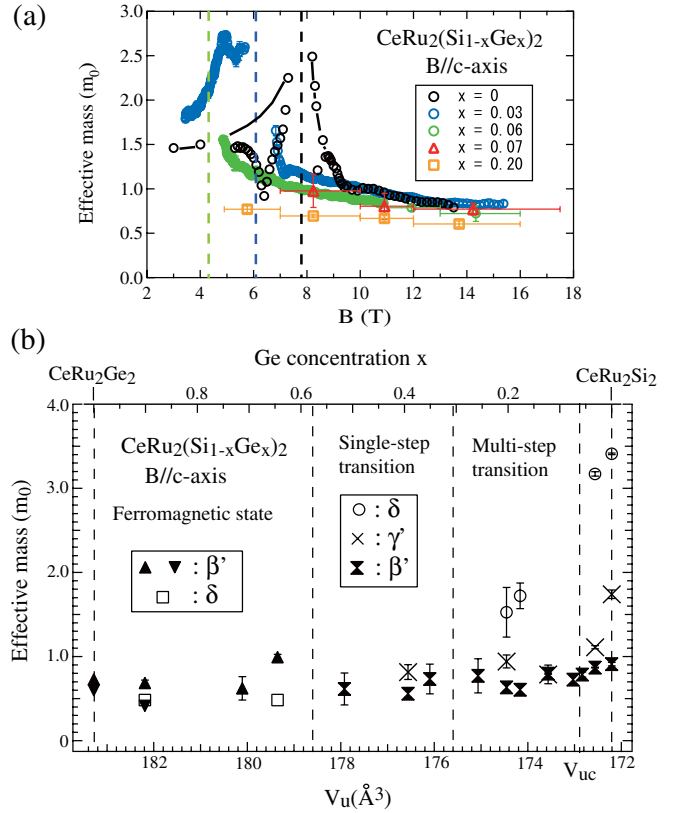


FIG. 4 (color). (a) Effective masses ( $m^*$ 's) in units of electron rest mass ( $m_0$ ) of the  $\beta$ - $\beta'$  oscillations plotted against  $B$  for CeRu<sub>2</sub>(Si<sub>1-x</sub>Ge<sub>x</sub>)<sub>2</sub> with  $x = 0, 0.03, 0.06, 0.07$  and  $0.20$ . The horizontal error bars denote the field range where the signal amplitudes are averaged. The solid lines are guides to the eye. The  $B_m$ 's for  $x = 0, 0.03$  and  $0.06$  are indicated by the broken lines. (b)  $m^*$ 's of the  $\beta'$ ,  $\gamma'$  and  $\delta$  oscillations plotted against unit cell volume ( $V_u$ ) or Ge concentration  $x$ . The values are obtained by the Fourier analysis in the field range between  $16$  T and  $10$  T. In the ferromagnetic state the field range between  $16$  T and  $8$  T was also used to determine the  $m^*$ 's of the up and down spin electrons separately.

In Fig. 4(b) we show the  $m^*$ 's above  $B_m$  and  $B_c$  as a function of  $V_u$ . The  $m^*$  of the  $\beta'$  oscillation does not vary much with  $V_u$  and seems to be slightly different between the up and down spin oscillations in the ferromagnetic state. Reliable values of the  $m^*$ 's of the  $\gamma'$  and  $\delta$  oscillations could not be obtained for some samples because of the low signal intensities. Particularly, since the  $F$ 's of the two oscillations are too close around  $V_{uc}$ , the  $m^*$ 's of  $\gamma'$  and  $\delta$  could not be determined separately in the same field range between  $10$  and  $16$  T. Analyses of the  $\gamma'$  and  $\delta$  oscillations in higher magnetic field ranges as well as in longer field ranges indicate that there is no signature of large mass enhancement near the  $V_{uc}$ . That is, they decrease with increasing  $V_u$  from CeRu<sub>2</sub>Si<sub>2</sub>. The behavior of  $m^*$  seems to correlate with that of the  $F$  change with  $V_u$ , i.e., when the changing rate of the  $F$  with  $V_u$  is large, that of  $m^*$  is also large. It seems to correlate also with the behavior

of  $T_m$  or  $T_K$ . The present observations for the  $F$  and  $m^*$  indicate that the FS properties change smoothly with  $V_u$  from above  $B_m$  in CeRu<sub>2</sub>Si<sub>2</sub> to CeR<sub>2</sub>Ge<sub>2</sub> and a drastic change of the FS properties takes place only in the narrow range of fields across  $B_m$ . One may assume that the orbits  $\beta$ ,  $\gamma$ , and  $\kappa$  deform and give rise to the  $\beta'$ ,  $\gamma'$ , and  $\delta$  oscillations above  $B_m$ , while keeping the FS volume the same. However, the differences in the  $F$ 's and  $m^*$ 's of these oscillations across  $B_m$  are comparable to or larger than those between above  $B_m$  in CeRu<sub>2</sub>Si<sub>2</sub> and CeRu<sub>2</sub>Ge<sub>2</sub> [1,3]. Therefore, as noted from Figs. 3 and 4, this assumption leads to an implausible conclusion that there are negligible changes in the FS properties compared with those across  $B_m$  even when the reconstruction of the FS takes place at a particular  $V_u$ .

The present magnetic phase diagram and the FS properties are interestingly compared with those of the cubic system CeIn<sub>3</sub>. It is found recently in CeIn<sub>3</sub> that in the polarized paramagnetic phase above the Néel ordered phase, the FS is that of the localized  $f$  electron [13]. On the other hand, in the paramagnetic phase above the critical pressure the FS is that of the itinerant  $f$  electron. Since there is no phase boundary intervening the two states outside of the closed phase boundary of the ordered phase on the  $B$ - $P$  plane, the transformation from the FS of itinerant  $f$  electron to that of localized  $f$  electron takes place in a continuous fashion in this region [13]. On the other hand, when we trace the FS properties from below  $B_m$  in CeRu<sub>2</sub>Si<sub>2</sub> to CeRu<sub>2</sub>Ge<sub>2</sub> by turning around the corner of the antiferromagnetic phase boundary, the FS also transforms from that of itinerant  $f$  electron to that of localized  $f$  electron. In contrast to CeIn<sub>3</sub>, CeRu<sub>2</sub>Si<sub>2</sub> has the strong Ising character and the rapid change like first-order transition from the paramagnetic heavy fermion state to the polarized state takes place across  $B_m$ . This is probably because the metamagnetic crossover is close to the first-order transition. Therefore, it is likely that a rather discontinuous transformation takes place across  $B_m$ , while the FS properties continue to transform smoothly with increasing  $V_u$  in the polarized state.

Finally, we discuss how the itinerant  $f$  electron state below  $B_m$  in CeRu<sub>2</sub>Si<sub>2</sub> can evolve to the localized and polarized state of CeRu<sub>2</sub>Ge<sub>2</sub> through the crossover. It is necessary to explain the drastic change of the FS properties across  $B_m$  together with rather continuous change of the electronic properties across  $B_m$  and the significant influence of the Kondo effect above  $B_m$ . Miyake and Ikeda [14] proposed a consistent explanation with the FS change from that of Fig. 1(a) to that of Fig. 1(b) across  $B_m$  based on the itinerant  $f$  electron model. In their model, so to say the quantum limit condition is reached for the strongly correlated flat band and consequently almost one  $f$  electron state per Ce is below the Fermi level and is polarized. Although

they assume fully hybridized bands above  $B_m$ , we think that the hybridization is much reduced above  $B_m$  owing to the magnetic field and the large magneto-volume effect [15]. We speculate that this  $f$  electron state can evolve continuously to that of CeRu<sub>2</sub>Ge<sub>2</sub>, but that the description of either localized or itinerant may not be adequate for this  $f$  electron state. On the other hand, Daou *et al.* assigns the  $\omega$  oscillation to the  $\mu$  orbit of Fig. 1(a) and claims that only the large hole surface of Fig. 1(a) reaches the quantum limit and the FS above  $B_m$  is that of the itinerant  $f$  electron surface [7]. However, we think that most of their arguments are not consistent with our previous experimental results [1,3].

In summary, the FS properties above the metamagnetic transitions in CeRu<sub>2</sub>(Si<sub>1-x</sub>Ge<sub>x</sub>)<sub>2</sub> evolve from above  $B_m$  to the ferromagnetic state of CeRu<sub>2</sub>Ge<sub>2</sub> without any discontinuous change. This continuous evolution is also consistent with the previous observations that the FS changes from that of Fig. 1(a) to that of Fig. 1(b) across  $B_m$  [1,3]. However, we conjecture that the nature of  $f$  electron may be ambiguous above  $B_m$  and may depend on the definitions of “itinerant” and “localized” under magnetic fields.

This work was supported by a Grant-in-Aid for Scientific Research from MEXT Japan.

- 
- [1] H. Aoki *et al.*, Phys. Rev. Lett. **71**, 2110 (1993).
  - [2] S.R. Julian *et al.*, Physica (Amsterdam) **199B & 200B**, 63 (1994).
  - [3] M. Takashita *et al.*, J. Phys. Soc. Jpn. **65**, 515 (1996).
  - [4] H. Yamgami and A. Hasegawa, J. Phys. Soc. Jpn. **62**, 592 (1993).
  - [5] H. Yamgami and A. Hasegawa, J. Phys. Soc. Jpn. **61**, 2388 (1992).
  - [6] S. Kambe *et al.*, Solid State Commun. **95**, 449 (1995).
  - [7] R. Daou C. Bergemann, and S.R. Julian, Phys. Rev. Lett. **96**, 026401 (2006).
  - [8] P. Haen *et al.*, Physica (Amsterdam) **259B & 261B**, 85 (1999).
  - [9] H. Wilhelm *et al.*, Phys. Rev. B **59**, 3651 (1999).
  - [10] R.A. Fisher *et al.*, J. Low Temp. Phys. **84**, 49 (1991).
  - [11] The measurement of  $B_m$  in CeRu<sub>2</sub>Si<sub>2</sub> under pressure gives a steeper slope of the  $B_m$  vs  $V_u$  curve, probably because the volume of the sample expands around  $B_m$ . Therefore, the extension of the results to negative pressure side led to the erroneous conclusion of our previous study [H. Aoki *et al.*, J. Phys. Soc. Jpn. **70**, 774 (2001)] that  $B_m$  reduces to zero at  $V_{uc}$ .
  - [12] M. Endo *et al.*, J. Phys. Soc. Jpn. **74**, 3295 (2005), and references therein.
  - [13] N. Harrison *et al.*, Phys. Rev. Lett. **99**, 056401 (2007).
  - [14] K. Miyake and H. Ikeda, J. Phys. Soc. Jpn. **75**, 033704 (2006).
  - [15] C. Paulsen *et al.*, J. Low Temp. Phys. **81**, 317 (1990).